Evaluation of Precise Point Positioning Using MADOCA-LEX via Quasi-Zenith Satellite System

Taro Suzuki, Nobuaki Kubo, Tomoji Takasu *Tokyo University of Marine Science and Technology, Tokyo, Japan*

BIOGRAPHIES

Taro Suzuki is a JSPS (Japan Society for the Promotion of Sciences) postdoctoral fellow at Tokyo University of Marine Science and Technology, Japan. He received his B.S., M.S., and Ph.D. in Engineering from Waseda University in 2007, 2009, and 2012 respectively. His current research interests include the GNSS precise positioning for vehicles integrated with inertial navigation and image sensors in urban environments. He also develops multipath mitigation techniques and an open source GNSS software receiver.

Nobuaki Kubo received his Master's degree of Electrical Engineering in 1998 from Hokkaido University. He received his doctorate in Engineering from University of Tokyo in 2005. He resided at Stanford University in 2008 as a visiting scholar. He is now an associate professor at the Tokyo University of Marine Science and Technology in the area of GPS/GNSS systems. His current interests are high accuracy automobile navigation using RTK and multipath mitigation techniques.

Tomoji Takasu is a research fellow of Laboratory of Satellite Navigation at Tokyo University of Marine Science and Technology. He was working for developments of satellite systems at NEC Aerospace systems Ltd. from 1984 to 1997. He is currently involved in the research and development of precise positioning algorithms with GPS/GNSS, including PPP, RTK and INS/GPS integration.

ABSTRACT

This paper describes the evaluation of precise point positioning (PPP) using the Quasi-Zenith Satellite System (QZSS) L-band Experiment (LEX) signal. The first QZSS, the Japanese regional satellite navigation system, was launched from Japan in September 2010. QZSS transmits augmentation signals to enhance the global navigation satellite system (GNSS) positioning accuracy. One of the QZSS augmentation signals is the LEX signal, the objective of which to realize centimeter-class positioning with its broadcasting data. The Japan Aerospace Exploration Agency began a test transmission of a MADOCA-LEX message, a new type of LEX message, in April 2013. MADOCA-LEX provides the satellite orbit and clock correction data of multi-GNSS using a state-space representation (SSR) format for real-time PPP. Unfortunately, the LEX signal cannot be received using the currently available commercial GNSS receivers. Moreover, for real-time applications, the LEX message contained in the LEX signal is required to be extracted for computing the user positions in real time. In this study, we have developed a novel technique for receiving and decoding the MADOCA-LEX message using a software GNSS receiver. We have developed a technique to decode the LEX messages without the use of an LEX signal tracking loop for estimating the code phase and the Doppler frequency of the LEX signal, however, with the aid of the conventional L1CA signal broadcasted simultaneously from the QZSS.
We have confirmed the effectiveness of the proposed method through static and kinematic tests. We have determined the receiver positions with a distance root-mean-square error of within 10 cm, by using PPP with the MADOCA-LEX message in the real-time static test. We have also found that the proposed localization technique is effective for position estimation with the decimeter-level accuracy through a kinematic test in the open-sky environment.

INTRODUCTION

Global navigation satellite systems (GNSSs) are rapidly gaining in popularity because of their wide range of current and potential applications. Examples of such applications include geodetic surveys and mappings, automatic vehicle navigations, and unmanned systems in autonomous construction machinery and precision agriculture. In these applications, high-precision satellite-based positioning constitutes a fundamental part of the application. In applications that require high-precision positioning in real time, a real-time kinematic (RTK) GPS/GNSS technique is usually used. RTK-GNSS is one of the most precise positioning technologies and can be

used to obtain centimeter-level accuracy of the position in real time by processing the carrier-phase measurements of GNSS signals [1-3]. RTK-GNSS is very popular; however, it requires GNSS base stations or simultaneous observations by dual-frequency GNSS receivers, which is inconvenient as cost is a consideration. In addition, the maximum distance between the user and the reference station must be less than 20 km because of the ionospheric error, which is dependent on the location [1]. Unlike the single-reference station RTK-GNSS approaches, where the positioning accuracy decreases as the baseline increases, the network RTK (NRTK) approaches ideally provide positioning with errors independent of the rover position within the network [4]. However, NRTK also requires a communication link and costs are involved to receive the correction data in many cases.

In recent years, precise point positioning (PPP) has been anticipated as an alternative to RTK-GNSS [5-7]. PPP can estimate a single-receiver position without any reference station or baseline through the use of satellite position fixes and clocks, which are predetermined. In comparison with the common techniques, the costs can be reduced. However, PPP requires fixed satellite positions and clocks, and the question of how to get these correction data remains. In this paper, we use the L-band Experiment (LEX) signal broadcasted by the Quasi-Zenith Satellite System (QZSS) to solve this problem. The first QZSS was launched from Japan in September 2010 [8-10]. The LEX signal broadcasted by QZSS is an augmentation signal, the objective of which is to realize centimeter-class positioning with its broadcasting data for the PPP. There are several types of LEX messages generated from several providers. The Japan Aerospace Exploration Agency (JAXA) began a test transmission of a MADOCA-LEX message, a new type of LEX message, in April 2013 [16-17]. The MADOCA-LEX message is designed to provide high-precision GPS and other GNSS satellite clock and ephemeris information for correcting the GNSS positioning error via the QZSS satellite in real time. Unfortunately, in 2013, the LEX signal could not be received using the currently available commercial GNSS receivers. Moreover, for real-time applications, the LEX message is required to be extracted for computing the user positions in real time.

In this study, we have developed a framework for PPP using a MADOCA-LEX message for real-time PPP. We have developed a novel technique for decoding the MADOCA-LEX message using a software GNSS receiver. The software GNSS receivers are widely recognized and used because of their configuration flexibility and ease of use in GNSS research [18-20]. Further, in this study, we have confirmed the position estimation capability in an actual outdoor environment by using real-time PPP with the QZSS MADOCA-LEX message.

QZSS OVERVIEW

In Japan, the first QZSS satellite named “MICHIBIKI,” the Japanese regional satellite navigation system, was launched in September 2010 [8]. The alert flags of its transmitting signals were dismissed in June 2011; a GNSS receiver corresponding to the QZSS could be used as QZSS for position calculations. Three additional QZSS satellites are commissioned to be launched by the end of 2017. The objective of QZSS is to enhance the availability and performance of the current GNSS positioning. Fig. 1 shows the orbit of the first QZSS satellite. The QZSS satellite is placed in highly inclined elliptical orbits. It causes an asymmetric “figure-eight” orbit, and hence, the elevation angle of the QZSS is greater than 75° for approximately 8 h/day in Tokyo, Japan. This has led to the coining of the term “quasi-zenith.” Further, we can receive the QZSS signal during most hours of the day even in dense urban environments where it is surrounded by tall buildings. QZSS broadcasts navigation signals such as L1CA, L2C, and L5. They are compatible with the modernized GPS signals and also used in interoperability. Furthermore, QZSS transmits augmentation signals to enhance the GNSS positioning accuracy. One of the QZSS augmentation signals is the LEX signal, the objective of which is to realize centimeter-class positioning with its broadcasting data.

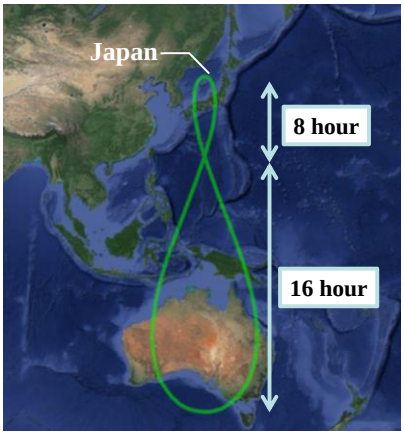

Fig. 1. Orbit of the first QZSS satellite (MICHIBIKI).

LEX SIGNAL

The LEX signal, an augmentation signal at the 1278.75-MHz band (same frequency as that of Galileo E6) broadcasted from QZSS, is anticipated to provide fine positioning up to the centimeter level [11,12,14]. The LEX message contained in this signal is designed to provide GPS and other GNSS satellite clock and ephemeris errors for correcting the GNSS positioning error via the QZSS satellite in real time. Fig. 2 shows the structure of the LEX message used for the broadcast of the augmentation information. The LEX message consists of a 49-bit header, 1695 bits of data, and 256 bits for error correction using the Reed–Solomon coding; the total size

of each message is 2000 bits [8]. The actual data transfer volume for the augmentation information is 1695 bps, with a basic structure of one message transmission per second. The augmentation information for entire Japan is required to be incorporated into 1695 bps. The LEX signal is overlaid by two ranging codes named "Short" and "Long" codes. In the case of the "Short" code, the period is 4 ms, and the code chip rate is 10,230 MChip/s. The LEX signal uses code shift keying (CSK) modulation. The CSK modulation shifts the phase of the LEX "Short" code by the number of chips indicated in the 8-bit encoded message symbol. In other words, the code phase difference between the original "Short" code and the transmitted "Short" code represents the LEX message symbol value in every 4 ms.

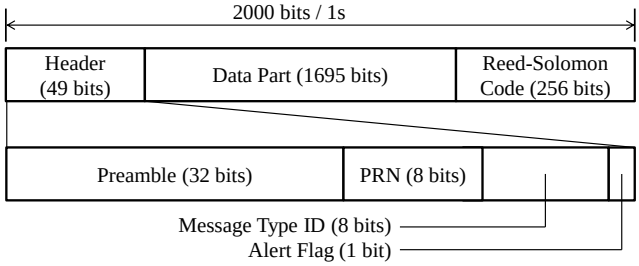

Fig. 2. Structure of the LEX message broadcasted by the QZSS LEX signal.

MADOCA-LEX MESSAGE

There are several types of LEX messages generated from several providers. The JAXA began a test transmission of a MADOCA-LEX message, a new type of LEX message, in April 2013. MADOCA, which stands for "Multi-GNNS Advanced Demonstration tool for Orbit-and-Clock Analysis," is the software developed by JAXA for estimating the orbits and clocks of currently available GNSS satellites with high precision [17]. JAXA prepared the multi-GNSS monitoring network (MGM-net) for collecting the multi-GNSS observation data in real time; 22 stations located around the world were operated in 2013. MADOCA uses the MGM-net to generate the multi-GNSS orbits and clocks by the collected multi-GNSS observation data at each station.

MADOCA-LEX provides the satellite orbit and clock correction data using a state-space representation (SSR) format for PPP [16]. The specification of MADOCA-LEX message is presented in Table 1. The MADOCA-LEX message contains the orbits, clocks, code biases, and user range accuracies (URAs), which are the statistical indicators of the GNSS ranging accuracy of GPS, GLONASS, QZSS, and Galileo. It is noted that, in January 2014, MADOCA-LEX contains only the GPS, GLONASS, and QZSS data; the Galileo correction information has not been broadcasted yet. The high rate clock data are updated every 2 s for high-speed corrections, and the orbit and URA data are updated every 30 s. The code bias data are updated every day for a low-speed correction item.

Table 1. Specification of the MADOCA-LEX message.

	SSR message number				Update interval
	GPS	GLO NASS	QZSS	Galileo	
Orbit	1057	1063	1246	1240	30 s
High Rate Clock	1062	1068	1251	1245	2 s
Code Bias	1059	1065	1248	1242	1 day
URA	1061	1067	1250	1244	30 s

PPP WITH LEX MESSAGE

PPP can estimate a single-receiver position without any reference station or baseline by setting the satellite positions and clocks to predetermined values. In addition, the estimated position is related to a well-defined geodetic datum, which is valid globally. Furthermore, PPP can be used for high-precision positioning without any baseline length limitation. For these reasons, PPP is anticipated to be a useful and efficient means for many localizing purposes [5-7]. The PPP technique is effective in many cases; however, it requires a communication link to obtain the correction data. When we use MADOCA-LEX broadcasted via QZSS, we can obtain a precise positioning solution by using the precise satellite orbit and clocks via the QZSS signal without the use of a communication link. Further, QZSS is suitable for broadcasting the augmentation information because QZSS has a high elevation angle, its signal is resistant to block by buildings even in an urban environment, and it is visible over long periods in Japan.

Fig. 3 shows an overview of the proposed PPP. MADOCA estimates the multi-GNSS orbits and clocks in real time using the MGM-net reference stations, and further, the estimated data are encoded, uplinked, and broadcasted via QZSS. As already mentioned, the

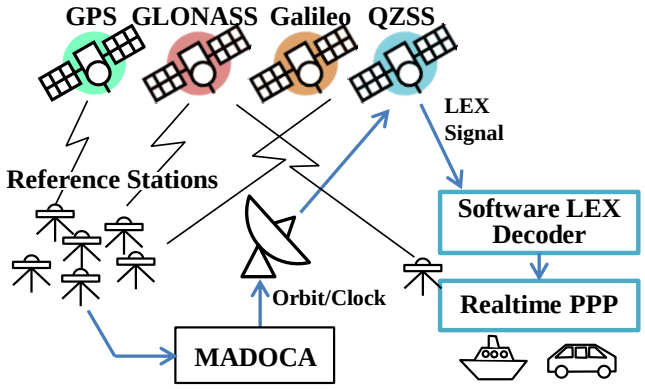

Fig. 3. Overview of the proposed PPP using the QZSS MADOCA-LEX message.

currently available commercial GNSS receivers cannot decode the LEX message. We have developed a QZSS LEX receiver that is able to decode the MADOCA-LEX message in real time using a software GNSS receiver technology. Finally, the PPP solutions with the MADOCA-LEX message are calculated in real time by RTKLIB, which is an open-source tool that can estimate the GNSS receiver position [7,11].

SOFTWARE LEX DECODER

Software GNSS receivers are widely recognized and used because of their configuration flexibility and ease of use in GNSS research [18-20]. In this paper, we develop a real-time LEX decoder based on the software GNSS receiver techniques [21]. The LEX signal uses CSK modulation. The CSK modulation shifts the phase of the LEX code by the number of chips indicated in the 8-bit encoded message symbol. The idea proposed in this paper is to decode the LEX messages without the LEX signal tracking loop for estimating the code phase and Doppler frequency of the LEX signal, however, with the aid of the conventional L1CA signal simultaneously broadcasted from the QZSS. Fig. 4 illustrates the LEX decoding algorithm using the QZSS L1CA signal. This algorithm requires a code phase and the Doppler information computed by the L1CA signal tracking result to extract the QZSS LEX message. The algorithm is executed as follows:

(i) First, the QZSS L1CA signal is acquired and tracked using the output of the GNSS radio-frequency (RF) front end. For the signal acquisition, a circular correlation based on fast Fourier transform (FFT) is used for estimating the rough Doppler frequency and the rough code phase of the L1CA signal for the initialization of the tracking loop [22]. In the tracking process, the accurate Doppler frequency and code phase are continuously estimated every 1 ms using the frequency lock loop (FLL), phase lock loop (PLL), and delay lock loop (DLL) [19]. During this time, the LEX "Short" code phase, which occurs every 4 ms, is unknown.

(ii) Further, the navigation bit overlaid in the L1CA code is synchronized. Upon synchronization of the navigation bit, the ambiguity of the original LEX "Short" code phase (nonshifted phase) can be resolved. We can then estimate the LEX Doppler frequency using the L1CA Doppler frequency. We denote the code phase as τ and the Doppler frequency as f. The code phase and Doppler frequency of the LEX signal are denoted using the L1CA signal as follows:

$$\tau_{LEX} = \tau_{L1CA} + \mathrm{D}_{\mathrm{L1CA-LEX}} \quad (1)$$

$$f_{LEX} = f_{L1CA}\frac{\mathrm{F}_{\mathrm{LEX}}}{\mathrm{F}_{\mathrm{L1CA}}} \quad (2)$$

The variable $\mathrm{D}_{\mathrm{L1CA-LEX}}$ is the bias of the code phases between the QZSS L1CA and the LEX signal, which is caused by the difference in the signal delay dependent on the frequency difference. We assume this difference as a constant value, and we have calibrated this value in advance. $\mathrm{F}_{\mathrm{L1CA}}$ and $\mathrm{F}_{\mathrm{LEX}}$ are signal frequencies of the L1CA and LEX signal. $\mathrm{F}_{\mathrm{L1CA}}$ and $\mathrm{F}_{\mathrm{LEX}}$ are 1575.42 and 1278.75 MHz, respectively.

(iii) Thereafter, the LEX code phase (the phase shifted on the basis of the CSK) is estimated using the FFT based on the circular correlation technique. We define the output of the RF front end as $S(t)$ and the LEX "Short code" as C_{LEX}. The shifted code phase in the frequency domain Z is calculated by the FFT using the code phase and Doppler frequency of the LEX signal as:

$$Z(\tau_{LEX}, f_{LEX}, S(t)) = \overline{\mathcal{F}[C_{LEX}]}\mathcal{F}\left[S(t-\tau_{LEX})e^{-j2\pi f_{LEX}t}\right] \quad (3)$$

where $\mathcal{F}[.]$ denotes the function of FFT. The shifted code phase in the time domain z is calculated using the following equation:

$$z = \left|\mathcal{F}^{-1}\left[Z(\tau_{LEX}, f_{LEX}, S(t))\right]\right|^2 \quad (4)$$

where $\mathcal{F}^{-1}[.]$ denotes the inverse FFT (IFFT). The LEX message symbol L can be calculated using the following equation:

$$L = \mathrm{N}_{\mathrm{LEX}} - z \quad (5)$$

where $\mathrm{N}_{\mathrm{LEX}}$ = 10,230 is the number of chips in the LEX code.

(iv) The error in the estimated message symbol L can be corrected by the Reed–Solomon code. The Reed–Solomon code used in the LEX message can correct a maximum of 16 symbol errors in each message (one message consists of 250 symbols). By using the Reed–Solomon code, the LEX message can be robustly decoded when the signal is weak in urban environments.

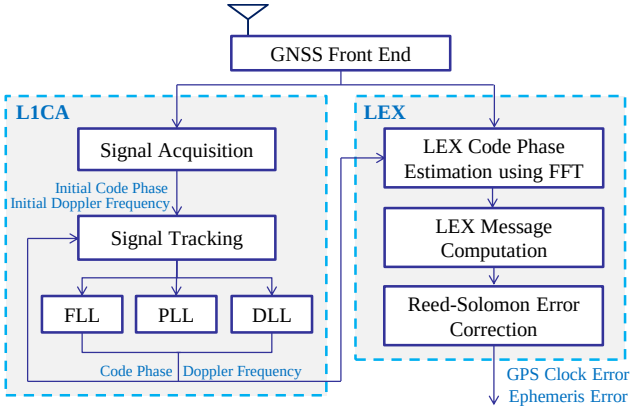

Fig. 4. Code phases of the L1CA and LEX signals obtained by the proposed method.

On the basis of the above, the GNSS satellite orbits and the clock can be extracted from the MADOCA-LEX message by using the software GNSS receiver, without tracking the LEX code []. We have conducted initial tests to evaluate the real-time decoding LEX message of the proposed method in an open-sky environment. Fig. 5 shows the estimated L1CA and LEX code phases by the proposed method. We have computed the LEX message symbol by taking the difference between the L1CA code phase and the LEX code phase described in equations (3)-(5). It is also determined that the shifted LEX code phases can be found every 4 ms. From this test, it has been concluded that it is possible to develop a method to receive the QZSS LEX message using the software GNSS receiver. In this test, we have used the laptop PC (Intel® Core™ i7-3635QM, 4 GB) to decode the LEX message in real time. The average computation time is approximately 1.8 ms to decode a 4-ms (1 symbol) LEX message. We have also confirmed that the proposed method can decode the LEX message in real time using a general-purpose PC. In the following section, we describe the real-time static and kinematic PPP using the QZSS MADOCA-LEX messages.

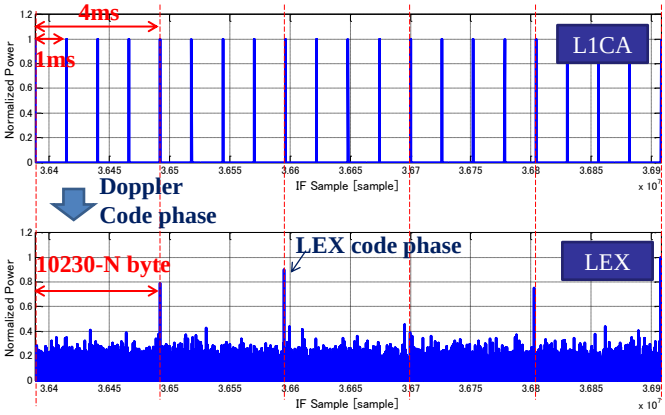

Fig. 5. Code phases of the L1CA and LEX signals obtained by the proposed method.

REAL-TIME PPP TEST IN A STATIC ENVIRONMENT

We have conducted a static test to evaluate our proposed method for position estimation using the real-time PPP with the QZSS MADOCA-LEX. We have compared the two positioning methods, which are (1) the MADOCA-LEX PPP using only GPS and (2) the MADOCA-LEX PPP using multi-GNSS (GPS, GLONASS, and QZSS). The test setup is shown in Fig. 6. We have used a front end (NSL Inc., Stereo version 2), GNSS antenna (Novatel Inc., 703-GGG), dual-frequency GNSS receiver (Javad Inc., GrAnt-G3T), and a laptop PC (Intel® Core™ i7-3635QM, 4GB) to decode the MADOCA-LEX message and calculate the real-time PPP solutions. The GNSS antenna has been installed at the rooftop of the building within the campus of the Tokyo University of Marine Science and Technology, Japan, and the antenna position has been predetermined using the conventional RTK-GNSS as the reference. Fig. 7 shows the fish-eye image captured at the antenna position in this test. The satellite positions actually received in this test are also projected onto the fish-eye image. The blue line shown in Fig. 7 indicates the QZSS satellite position. It can be determined that the test environment is an open-sky environment, and the signals from QZSS and other GNSS can be tracked continuously during the test.

We have conducted two static tests under the same conditions. Table 2 summarizes the description of the two tests. Test #1 was performed for 18 h from 1/16/2014 to 1/17/2014, and test #2 was performed for 18 h from 1/17/2014 to 1/18/2014. The real-time PPP solutions have been calculated at a rate of 1 Hz and stored in the PC.

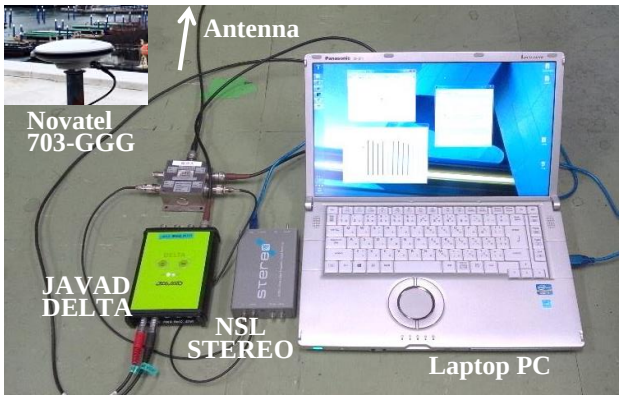

Fig. 6. Configuration of the real-time static PPP test.

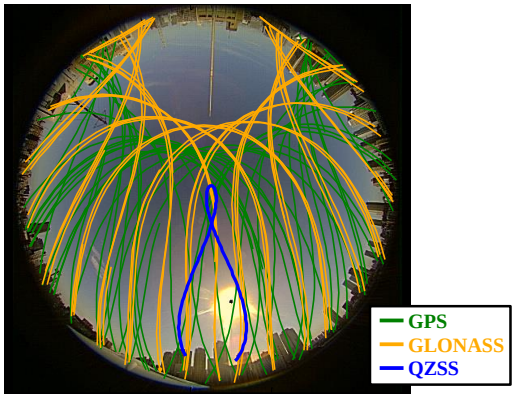

Fig. 7. Fish-eye image and satellite constellation during the test.

Table 2. Description of the static PPP test.

Test	Start	Stop	Per-iod	Enviro-nment	PPP Mode
#1	1/16 /2014, 15:00	1/17 /2014, 11:00	18 h	Open sky	Kinematic, GPS/Multi-GNSS
#2	1/17 /2014, 15:00	1/18 /2014, 11:00	18 h	Open sky	Kinematic, GPS/Multi-GNSS

The horizontal positioning error and the time-series positioning error in the east, north, and up directions in Test #1 and Test #2 are illustrated in Fig. 8 and Fig. 9, respectively. In these figures, the blue lines indicate the error in PPP using GPS, and the green lines indicate the error in PPP using multi-GNSS. It is noted that PPP requires the convergence time to estimate the accurate user position. In this test, the position solutions in the first 1 h are ignored to evaluate the statistical value. The evaluation of the convergence time is discussed in the next section. The standard deviation (SD), root mean square (RMS), and maximum errors in the real-time PPP using the MADOCA-LEX message in the static test are listed in Table 3. The horizontal RMS errors in Test #1 and #2 are 7.1 cm and 8.6 cm, respectively, using GPS. In contrast, the horizontal RMS errors are improved to 5.0 cm and 5.1 cm, respectively, using multi-GNSS PPP. It can be determined that the positioning accuracy of the real-time MADOCA-LEX PPP in an open-sky environment is within 10 cm. MADOCA-LEX also realizes centimeter-class positioning in real time with the QZSS broadcasting data for the PPP.

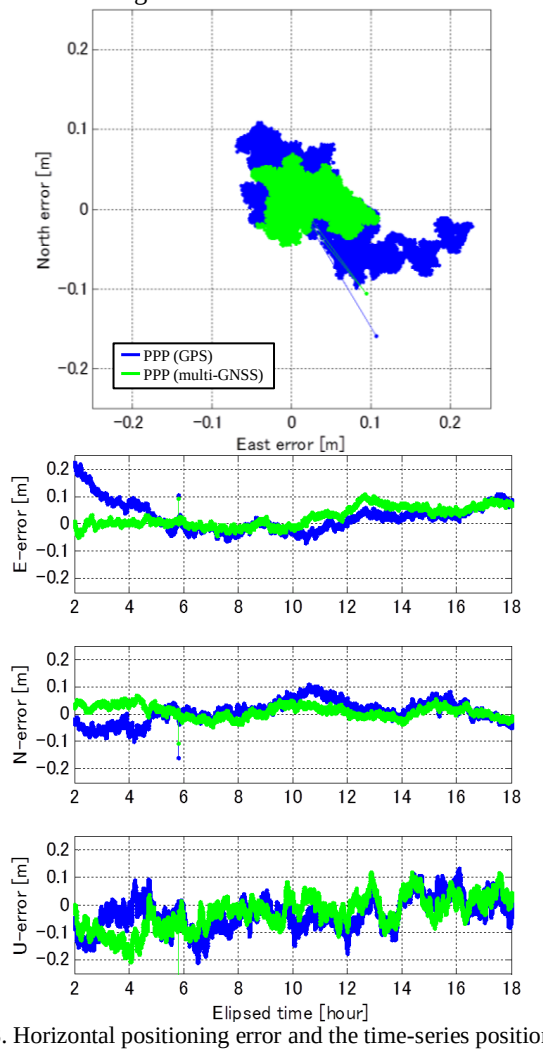

Fig. 8. Horizontal positioning error and the time-series positioning error in the east, north, and up directions in Test #1 (static and open-sky environment).

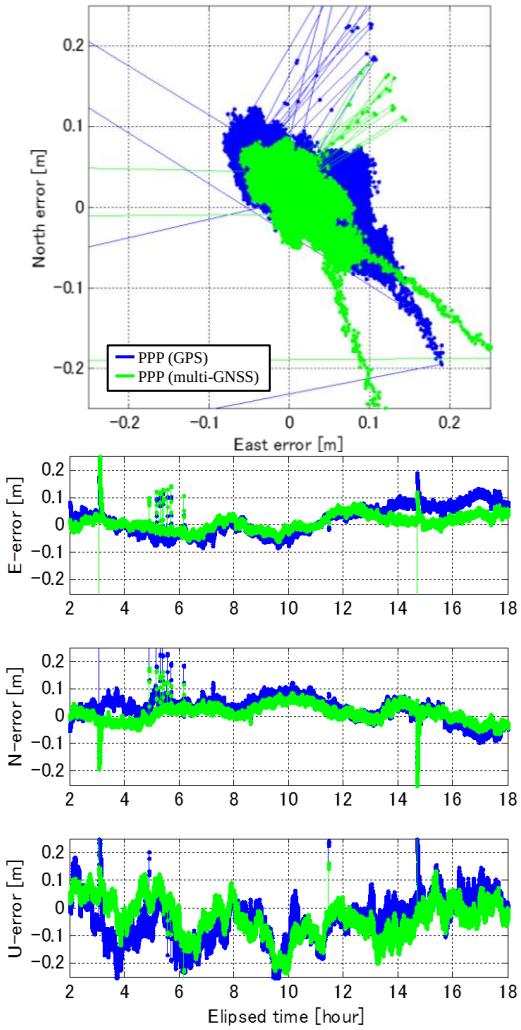

Fig. 9. Horizontal positioning error and the time-series positioning error in the east, north, and up directions in Test #2 (static and open-sky environment).

Table 3. Horizontal positioning errors in the static tests using MADOCA LEX-PPP.

Horiz-ontal error	Test #1		Test #2	
	GPS	Multi-GNSS	GPS	Multi-GNSS
SD	3.9 cm	2.2 cm	4.9 cm	3.0 cm
RMS	7.1 cm	5.0 cm	8.6 cm	5.1 cm
Max.	22.7 cm	14.1 cm	160.7 cm	79.3 cm

Further, we have evaluated the convergence time of the PPP using the MADOCA-LEX. Fig. 10 shows the horizontal RMS error in the first 30 m in the static test for comparing the performance of the convergence time. The blue and green lines shown in Fig. 10 are the horizontal errors in PPP using GPS and multi-GNSS, respectively.

The light blue and pink lines indicate the 3-sigma SD of the solutions calculated in the process of PPP by the Kalman filter. The PPP using GPS requires a long convergence time when compared with that using multi-GNSS. Table 4 summarizes the convergence time versus the horizontal accuracy. In Test #2, the PPP using GPS required over 4000 s to achieve the 0.2-m horizontal position accuracy. It is observed from this evaluation that the MADOCA-LEX PPP using multi-GNSS has an advantage in terms of the convergence time when compared with that using only GPS.

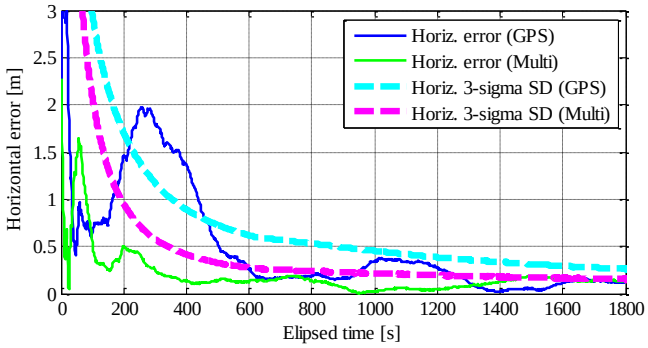

Fig. 10. Comparison of the convergence time of the PPP.

Table 4. Comparison of the convergence time of the PPP.

Horiz-ontal error	Test #1		Test #2	
	GPS	Multi-GNSS	GPS	Multi-GNSS
< 1 m	35 s	7 s	26 s	18 s
< 0.5 m	504 s	102 s	180 s	112 s
< 0.2 m	617 s	325 s	4150 s	212 s

REAL-TIME PPP TEST IN A KINEMATIC ENVIRONMENT

We have also conducted a kinematic vehicle test to evaluate our proposed method for position estimation using the real-time PPP with the QZSS MADOCA-LEX. The test setup is the same as that of the static test introduced in the previous section. In the case of the vehicle test, the antenna has been installed on the roof of the vehicle. Fig. 11 shows the sensor configurations and the vehicle used in this test. In order to compare the positioning accuracy with the results obtained by the proposed PPP, we have used the RTK-GNSS fix solutions as the reference positions. However, an RTK-GNSS fix solution cannot be obtained when the number of satellites is reduced in an actual kinematic environment. Therefore, we have also installed a fiber-optic gyroscope (FOG) and wheel encoder for measuring the orientation and velocity of the vehicle. We have combined the RTK-GNSS fix solutions and dead reckoning (DR) results using the Kalman filter along with the FOG and the wheel encoder to generate the reference path.

We have conducted two kinematic tests under the open-sky and urban environments. Table 5 summarizes the description of the two tests. Test #1 was performed for 1.5 h on 1/24/2014 in an open-sky environment, and test #2 was performed for 1.2 h on 1/24/2014 in an urban environment. Fig. 12 shows the time series of the fish-eye images showing the course environment in the open-sky and urban environments, respectively. In the case of Test #2, the urban environment test, the surroundings of the travel route consisting of some buildings, making it an environment susceptible to satellite masking. There were many instances where the number of satellites was decreased because of obstruction by the buildings. However, in both the open-sky and urban tests, the QZSS had a high elevation angle, and therefore, we could receive the signal from the QZSS even when the vehicle was in an urban area.

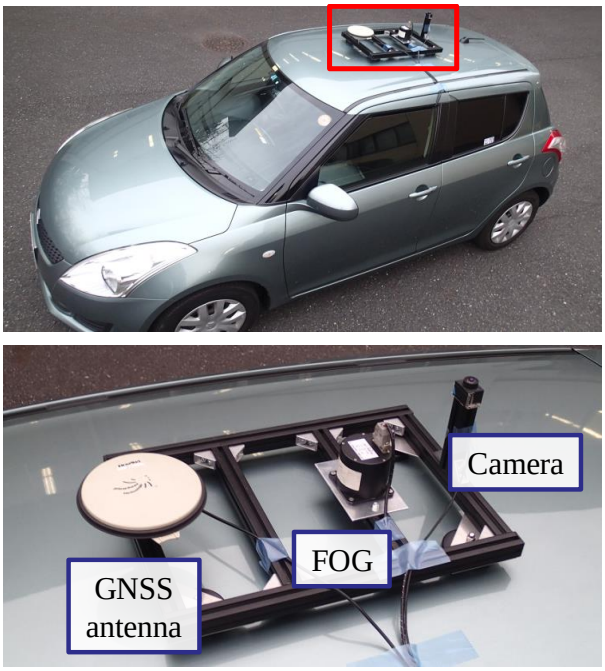

Fig. 11. Sensor configurations and the vehicle used in this test.

Table 5. Description of the static PPP test.

Test	Start	Stop	Per-iod	Enviro-nment	PPP Mode
#1	1/24 /2014, 0:30	1/24 /2014, 2:30	1.5 h	Open sky	Kinematic, GPS/ Multi-GNSS
#2	1/24 /2014, 4:00	1/24 /2014, 5:12	1.2 h	Urban	Kinematic, GPS/ Multi-GNSS

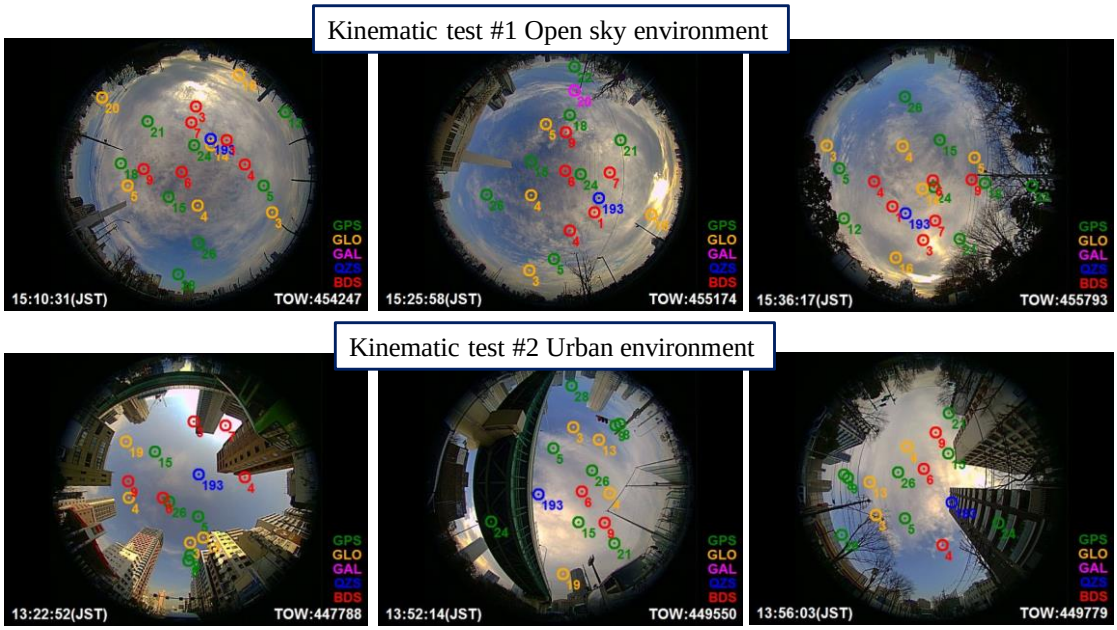

Fig. 12. GPS and QZSS satellite constellation during the test.

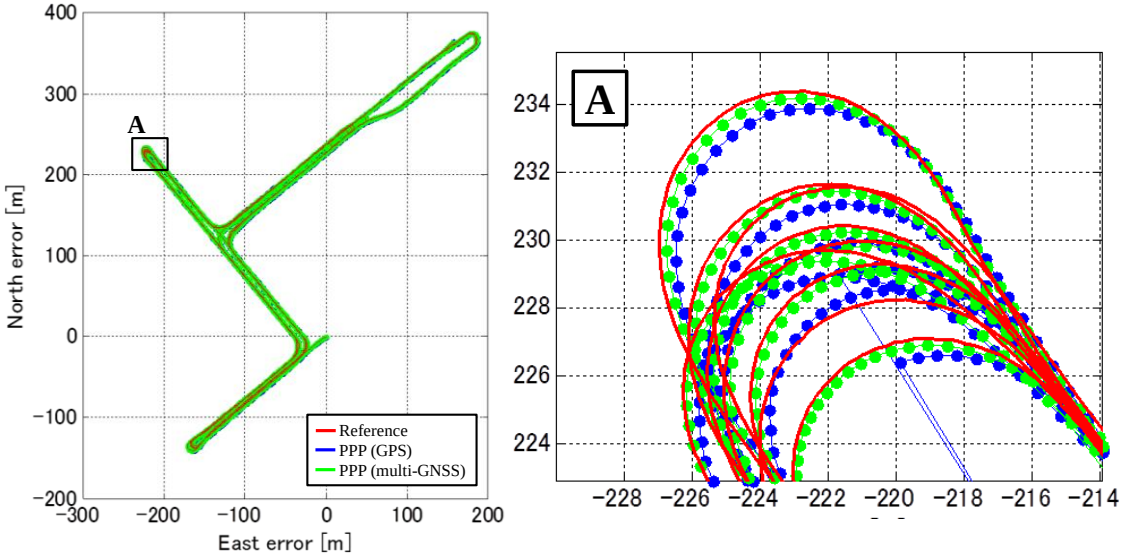

Fig. 13. Comparison of the positions estimated by the MADOCA-LEX PPP of Test #1 (kinematic and open-sky environment).

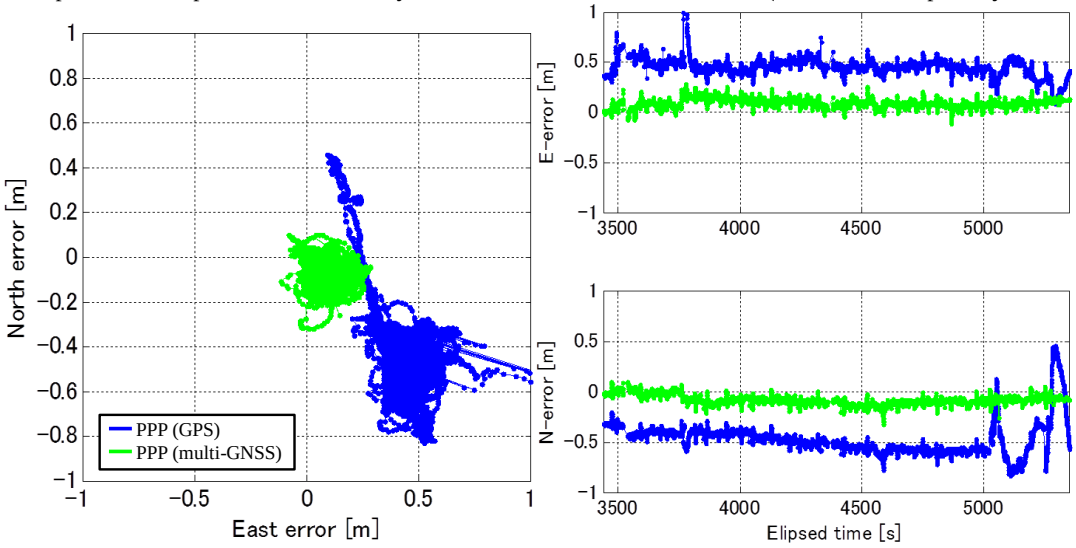

Fig. 14. Horizontal positioning error and the time-series positioning error in Test #1 (kinematic and open-sky environment).

kinematic test in the open-sky environment. The estimated horizontal vehicle position of Test #1 is illustrated in Fig. 13. "A" in Fig. 13 shows a close-up view of the entire estimated positions. The red line denotes the reference paths computed by the RTK-GNSS and DR, the blue line denotes the PPP solutions using GPS, and the green line denotes the PPP solutions using multi-GNSS. The horizontal positioning error and the time-series positioning error in the east and north directions in Test #1 are illustrated in Fig. 14. These errors are computed using the reference path shown in Fig 13. In the result of the PPP using GPS, the bias error remains; however, the MADOCA-LEX PPP using multi-GNSS indicates a good positioning accuracy (within 20 cm) even in the kinematic test.

Further, we have compared the localization results of the kinematic test in the urban environment. The estimated horizontal vehicle position in Test #2 is illustrated in Fig. 15. The red line denotes the reference paths computed by the RTK-GNSS and DR, the blue line denotes the PPP solutions using GPS, and the green line denotes the PPP solutions using multi-GNSS. As shown in Fig. 15, both the estimated positions are discontinuous and jump at position "A" because of the multipath effects. In this environment, there were many instances where the tracking signals were discontinuous, and carrier phase cycle slips occurred because of obstruction by the buildings. The horizontal positioning error and the time-series positioning error in the east and north directions in Test #2 are illustrated in Fig. 16. This figures show that both the positioning results are very noisy when compared to that shown in Fig. 14, which is the result of the open-sky kinematic test.

The SD, RMS, and maximum errors in the PPP solutions using the MADOCA-LEX message in the kinematic test are summarized in Table 6. The horizontal RMS errors in Test #1, the open-sky environment test, are 0.68 m and 0.14 m in the case of using GPS and using multi-GNSS, respectively. By using multi-GNSS PPP, the positioning accuracy can be improved in the open-sky kinematic test. In contrast, the horizontal RMS errors in Test #2, the urban environment test, are 3.4 m and 2.2 m using GPS

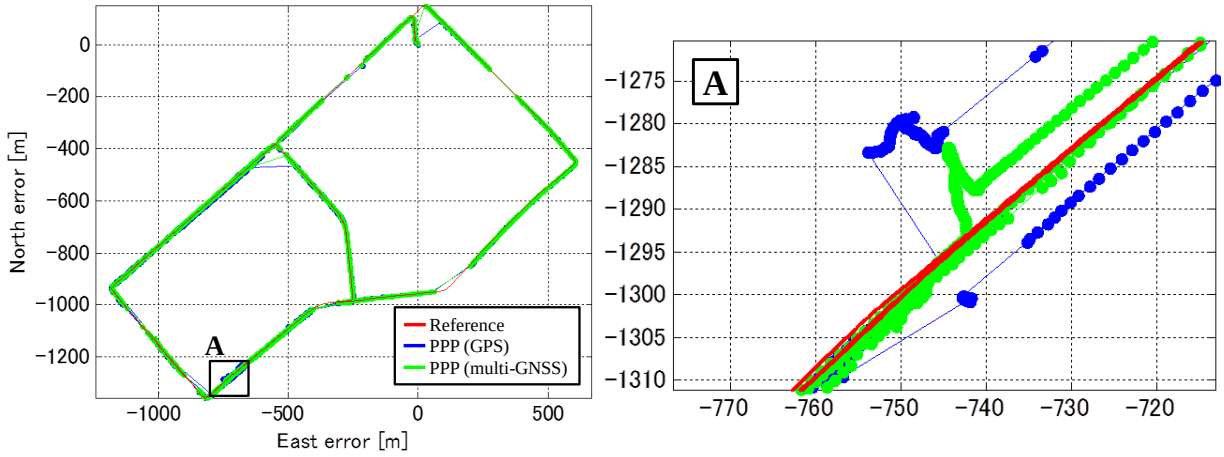

Fig. 15. Comparison of the positions estimated by the MADOCA-LEX PPP in Test #2 (kinematic and urban environment).

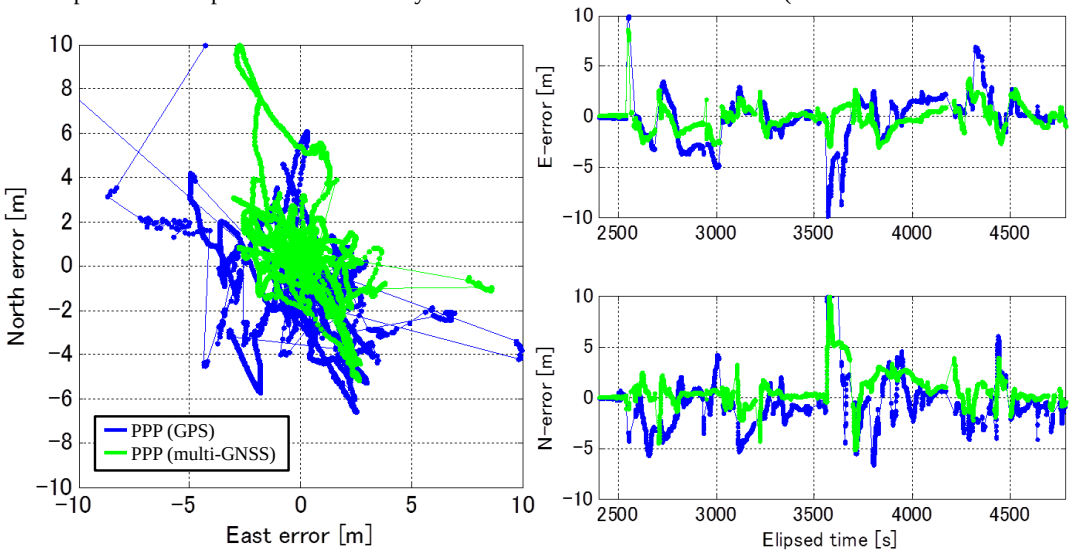

Fig. 16. Horizontal positioning error and the time-series positioning error in Test #2 (kinematic and urban environment).

and using multi-GNSS, respectively. It can be determined that the positioning accuracy of the real-time MADOCA-LEX PPP in the kinematic test is decimeter-class in the open-sky environments. It is also confirmed that the MADOCA-LEX PPP is difficult to use in urban environments because of the multipath and carrier cycle slips. These results show that our proposed method, real-time PPP using QZSS MADOCA-LEX, effectively estimates the position with high precision in open-sky environments. Our experiments have demonstrated the feasibility of high-precision position estimation with a single GNSS receiver using the QZSS MADOCA-LEX messages.

Table 6. Horizontal positioning errors in kinematic tests using MADOCA LEX-PPP.

Horiz-ontal error	Test #1 (Open sky)		Test #2 (Urban)	
	GPS	Multi-GNSS	GPS	Multi-GNSS
SD	0.13 m	0.04 m	2.27 m	1.52 m
RMS	0.68 m	0.14 m	3.43 m	2.23 m
Max.	1.32 m	0.32 m	15.69 m	10.37 m

CONCLUSION

In this paper, we proposed a PPP technique using a QZSS MADOCA-LEX message for real-time localization purposes. PPP can estimate a single-receiver position without any reference station, and it is therefore expected to be a means for localization of many applications. MADOCA-LEX provides precise satellite orbit and clock correction data of multi-GNSS for real-time PPP. We developed an algorithm for a software GNSS receiver to receive the QZSS MADOCA-LEX message with the aid of the conventional L1CA signal broadcasted simultaneously from the QZSS. We confirmed the usefulness of this technique through comparison between the static and the kinematic tests conducted in actual outdoor environments. We could determine the receiver positions with a horizontal RMS error of within 10 cm, by using the PPP with the MADOCA-LEX message in the real-time static test. We also found that the proposed localization technique is effective for position estimation with the decimeter-level accuracy through a kinematic test in an open-sky environment.

A future challenge is to mitigate the multipath effect using the satellite selection technique. In addition, the all-cycle slips caused by the satellite masking must be found in real time. We expect that the positioning accuracy can be further improved by the determination of the multipath signals and cycle slips in urban environments. Furthermore, we will evaluate the proposed localization method in a wide range of outdoor kinematic environments.

ACKNOWLEDGMENTS

This work was supported by Grant-in-Aid for Japan Society for the Promotion of Science (JSPS) Fellows.

REFERENCES

[1] Kaplan, E. and Hegarty, C., Understanding GPS: Principles and Applications, 2nd Edition, Artech House, Boston, 2005.

[2] Leick, A., “GPS Satellite Surveying,” 3rd Edition, John Wiley & Sons, Inc., Hoboken, New Jersey, USA, 2004.

[3] S. Thrun, et al., “Stanley, the robot that won the DARPA Grand Challenge”, Journal of Field Robotics, Vol. 23, No. 9, pp. 661–692, 2006.

[4] Lachapelle, G., Alves, P., Fortes, LP., Cannon, ME. and Townsend, B., “DGPS RTK positioning using a reference network,” Proc. of ION ITM 2000, pp. 1165–1171, 2000.

[5] Zumberge, J. F., Heflin, M. B.: Jefferson, D. C. and Watkins, M. M., “Precise point positioning for the efficient and robust analysis of GPS data from large networks,” Journal of Geophysical Research 102(B3), pp. 5005-5017, 1997.

[6] Morales, Y. and Tsubouchi, T., “DGPS, RTK-GPS and StarFire DGPS Performance Under Tree Shading Environments,” Proc. of the IEEE International Conference on Integration Technology, pp.519-524, 2007.

[7] T. Takasu, “Real-time PPP with RTKLIB and IGS real-time satellite orbit and clock,” IGS Workshop 2010.

[8] Japan Aerospace Exploration Agency, “Quazi-Zenith Satellite System Navigation Service, Interface Specification for QZSS (IS-QZSS) Version 1.5” Technical report, 2013.

[9] A. Hauschild, P. Steigenberger, and C. RodriguezSolano, “Signal, orbit and attitude analysis of Japan’s first QZSS satellite Michibiki,” GPS Solutions, 16(1), pp. 127–133, 2012.

[10] M. Kishimoto, E. Myojin, S. Kogure, H. Noda, and K. Terada, “QZSS On Orbit Technical Verification Results,” Proc. of ION GNSS 2011, 2011.

[11] T. Takasu, “Real-Time PPP Experiment via QZSS LEX and its Extension,” Proc. of International Symposium on GPS/GNSS, 2010.

[12] Saito M, Sato Y, Miya M, Shima M, Omura Y, Takiguchi J, Asari K, “Centimeter-class augmentation system utilizing Quasi-Zenith Satellite,” Proc. ION GNSS 2011, Portland, Oregon, 19-23 September, pp.1243-1253, 2011.

[13] Wu, J., Lei, B., Dempster A. G., Rizos, C., “QZSS LEX Receiver Design,” Proc. of International Global Navigation Satellite Systems Society (IGNSS) Symposium 2013, 2013.

[14] Suelynn Choy, et al., “Real-Time Precise Point Positioning Utilising the Japanese Quasi-Zenith Satellite System (QZSS) LEX Corrections,” Proc. of International Global Navigation Satellite Systems Society (IGNSS) Symposium 2013, 2013.

[15] Kenji Nakakuki, Rui Hirokawa, “An Efficient Acquisition Method for the CSK Signal of QZSS LEX,” Proc. of ION GNSS 2013, 2013.

[16] Japan Aerospace Exploration Agency, “MADOCA-LEX format (Provisional)”, 2013.

[17] T. Takasu, “Development of Multi-GNSS Orbit and Clock Determination Software MADOCA,” The 5th Asia Oceania Regional Workshop on GNSS, December 1-3, 2013.

[18] K. Borre, D. M. Akos, et al. “A Software-Defined GPS and Galileo Receiver: A Single-Frequency Approach”, Springer, New York, 2007.

[19] James B.Y. Tsui, “Fundamentals of Global Positioning System Receivers: A Software Approach,” Second Edition, Wiley, 2005.

[20] S. Zhao, D. Akos, “An Open Source GPS/GNSS Vector Tracking Loop -Implementation, Filter Tuning, and Results,” in Proc. of ION ITM 2011, pp. 1293 – 1305, 2011.

[21] GNSS-SDRLIB: an open source GNSS software defined radio library, http://www.taroz.net/gnsssdrlib_e.html

[22] David M. Lin, and James B.Y. Tsui, “Comparison of Acquisition Methods for Software GPS Receiver,” Proc. of ION GPS 2000, 2000.